

Charge ordering and chemical potential shift in $\text{La}_{2-x}\text{Sr}_x\text{NiO}_4$ studied by photoemission spectroscopy

M. Satake, K. Kobayashi

Department of Physics, University of Tokyo, Bunkyo-ku, Tokyo 113-0033, Japan

T. Mizokawa, A. Fujimori*

*Department of Physics and Department of Complexity Science and Engineering,
University of Tokyo, Bunkyo-ku, Tokyo 113-0033, Japan*

T. Tanabe, T. Katsufuji and Y. Tokura

Department of Applied Physics, University of Tokyo, Bunkyo-ku, Tokyo 113-0033, Japan

(October 15, 2018)

We have studied the chemical potential shift in $\text{La}_{2-x}\text{Sr}_x\text{NiO}_4$ and the charge ordering transition in $\text{La}_{1.67}\text{Sr}_{0.33}\text{NiO}_4$ by photoemission spectroscopy. The result shows a large (~ 1 eV/hole) downward shift of the chemical potential with hole doping in the high-doping regime ($\delta \gtrsim 0.33$) while the shift is suppressed in the low-doping regime ($\delta \lesssim 0.33$). This suppression is attributed to a segregation of doped holes on a microscopic scale when the hole concentration is lower than $\delta \simeq 1/3$. In the $\delta = 1/3$ sample, the photoemission intensity at the chemical potential vanishes below the charge ordering transition temperature $T_{\text{CO}} = 240$ K.

Recently charge ordering phenomena in transition-metal oxides have attracted considerable interest, particularly due to the possible relationship between charge stripes and high-temperature superconductivity in the cuprates or giant magnetoresistance in the manganites. Charge ordering in a stripe form in the nickelates $\text{La}_{2-x}\text{Sr}_x\text{NiO}_4$ has been well established experimentally¹ and theoretically² while it is more controversial in the cuprates, e.g., $\text{La}_{2-x-y}\text{Nd}_y\text{Sr}_x\text{CuO}_4$ with $x \simeq \frac{1}{8}$.³ In $\text{La}_{2-x}\text{Sr}_x\text{CuO}_4$, charge stripes, if exist, are dynamical, half-filled with holes and run along the Cu-O bond directions, whereas in $\text{La}_{2-x}\text{Sr}_x\text{NiO}_4$ they are static, filled with holes, and run along the diagonal Ni-Ni directions. In order to characterize the behaviors of the stripe fluctuations in the cuprates and to elucidate their relationship to the superconductivity, it is important to study the well characterized case of the nickelates in more detail. It has been established that the charge ordering in the diagonal stripe form in $\text{La}_{2-x}\text{Sr}_x\text{NiO}_4$ is most stable at $x \simeq 0.33$.^{1,4-6} For this composition, neutron scattering studies have shown that charge ordering occurs below $T_{\text{CO}} \simeq 240$ K and antiferromagnetic ordering occurs below $T_{\text{N}} = 190$ K.⁵ Electrical resistivity shows a steep increase below T_{CO} .⁴

In this paper, we report on a photoemission study of the chemical potential shift in $\text{La}_{2-x}\text{Sr}_x\text{NiO}_4$ as a function of hole concentration and the temperature dependence of photoemission spectra across the phase transitions for $x = 0.33$. The shift of the electron chemical potential μ as a function of electron density n is related to the charge compressibility κ or the charge susceptibility χ_c through $\kappa = (1/n^2)(\partial n/\partial \mu)$ or $\chi_c = \partial n/\partial \mu$ and can be measured through the shifts of spectral features in photoemission spectra since binding energies in the photoemission spectra are experimentally referenced to the

chemical potential μ , namely, the Fermi level. The chemical potential shift has been studied for $\text{La}_{2-x}\text{Sr}_x\text{CuO}_4$ (LSCO) and found to be suppressed in the underdoped region $x \lesssim 0.15$.⁷ The suppressed chemical potential shift, or equivalently the enhanced charge compressibility, in spite of the reduced density of states at the chemical potential as measured by the electronic specific heat,⁹ has been interpreted as due to the opening of a pseudogap or to a microscopic phase separation.⁷ Indeed, such a pseudogap opening has been confirmed by a subsequent angle-resolved photoemission study of LSCO.⁸

Single crystals of $\text{La}_{2-x}\text{Sr}_x\text{NiO}_{4+y/2}$ (LSNO) were prepared by the floating zone method. Hole concentration $\delta = x + y$ except for the $x = 0$ sample was determined by iodimetric titration with an accuracy of ± 0.01 . The chemical compositions thus determined are tabulated in Table I. X-ray photoemission spectroscopy (XPS) measurements were performed using a spectrometer equipped with a Mg $K\alpha$ source ($h\nu = 1253.6$ eV) and a PHI double-pass cylindrical-mirror analyzer. The energy resolution including the x-ray source and the analyzer was ~ 1.0 eV but we could determine the shifts of core levels to an accuracy of ± 50 meV as in the case of LSCO.⁷ Binding energies were calibrated using Au evaporated on the samples. All the XPS spectra were taken at liquid-nitrogen temperature (~ 77 K). High-resolution ultraviolet photoemission spectroscopy (UPS) measurements were carried out using a He I resonance line ($h\nu = 21.2$ eV) and VSW and Omicron 125-EA hemispherical analyzers. The He I spectra have been corrected for the He I* satellite. In order to determine the Fermi level (E_F) and to estimate the instrumental resolution, Au was evaporated on each sample. The energy resolution was estimated to be 25-30 meV. The sample surfaces were repeatedly scraped *in situ* with a diamond file to obtain clean

surfaces. The cleanliness of the surfaces was checked by lack of contamination/degradation-related features on the higher binding-energy side of the O 1s peak in the XPS spectra or that at ~ -4.5 and ~ -9 eV in the UPS spectra.

Figure 1 shows the XPS spectra of the O 1s and La $3d_{5/2}$ core levels taken at liquid-nitrogen temperature. The vertical lines indicate the estimated positions of the core levels. As for the La $3d_{5/2}$ peak, the shift was estimated from the position at half peak height on the lower-binding-energy side of the peak because the effect of surface degradation appears on the higher-binding-energy side. Estimated shifts of the O 1s and La $3d$ spectra are plotted in Fig. 1(c). Now, we can assume that the shifts of the O 1s and La $3d$ core levels are largely due to the shift of the chemical potential as in the case of LSCO⁷ for the following reasons. First, the identical shifts of the O 1s and La $3d$ spectra with δ indicate that the effect of changes in the Madelung potential caused by the $\text{La}^{3+} \rightarrow \text{Sr}^{2+}$ substitution can be neglected. This is because the changes in the Madelung potential would cause shifts of the core levels of the O^{2-} anion and the La^{3+} cation in the opposite directions if this effect were significant. Second, changes in the number of electrons of the O and La atoms with hole concentration, which may cause shifts of the La and O core levels, can also be neglected. Unfortunately, it was not possible to measure the shift of the Ni 2p core level with sufficient accuracy because the Ni $2p_{3/2}$ peak was overlaid by the La $3d_{3/2}$ peak and the Ni $2p_{1/2}$ peak was too broad.

The valence-band spectra of LSNO with various hole concentrations $\delta = x + y$ were also measured using UPS as shown in Fig. 2(a) and the spectral shift was deduced in the same way. All the spectra were taken at 150 K except for $\delta = 0$, whose spectrum was measured at 230 K to avoid charging effect. These spectra have been normalized to the peak height at ~ -3 eV. The shift was estimated from the non-bonding O $2p$ peak at ~ -3 eV because its electronic state should be insensitive to the hole concentration compared to the $d^8\bar{L}$ final states at ~ -1.5 eV. In order to avoid the effect of surface degradation, which appear at ~ -4.5 eV, the shift of the O $2p$ peak was estimated from the position at 3/4 peak height on the lower-binding-energy side of the peak as indicated by vertical lines in Fig. 2(a). Figure 2(b) shows the shift of the O $2p$ peak thus evaluated. The shift of the non-bonding O $2p$ peak should represent the chemical potential shift $\Delta\mu$ in the same way as that of the O 1s peak. Indeed, $\Delta\mu$ deduced from the shift of the O $2p$ levels and that deduced from the average shift of the O 1s and La $3d$ levels agree with each other as shown in Fig. 3(a), where $\Delta E_{\text{O}2p}$, $\Delta E_{\text{O}1s}$, and $\Delta E_{\text{La}3d}$ are changes in the binding energies of the O $2p$, O 1s, and La $3d$ levels, respectively.

The sign of $\Delta\mu$ is consistent with the downward shift as expected for hole doping. However, the suppression of the shift for $0 \leq \delta \leq 0.30$ cannot be explained within a rigid-band picture because the chemical potential μ in an insulator would shift rapidly with hole doping in the

rigid-band picture. Therefore, this non-rigid-band behavior implies remarkable correlation effects in LSNO. Such a suppression of $\Delta\mu$ has also been found in LSCO as shown in Fig. 3(b),⁷ where μ shows a large (~ 1.5 eV/hole) downward shift with hole doping in the overdoped ($x \gtrsim 0.15$) region and a small (< 0.2 eV/hole) shift in the underdoped ($x \lesssim 0.15$) region. In LSNO, μ shows a large (~ 1.5 eV/hole) downward shift for $\delta \gtrsim 0.33$ and a small (< 0.2 eV/hole) shift for $\delta \lesssim 0.33$. The low-doping region of $x \lesssim 0.33$ in the nickelates is thus analogous to the underdoped region of $x \lesssim 0.15$ in the cuprates. Since LSCO is considered to show dynamical stripe fluctuations according to the inelastic neutron scattering studies,¹⁰ it is likely that the pinning of μ below the critical hole concentration is a common phenomenon for stripe formation. The following scenario may be considered as a common mechanism for the pinning of μ . Charge ordering in a stripe form is a kind of “phase separation” into a hole-rich region and a hole-poor region on a microscopic length scale. The hole chemical potential $-\mu$ (where μ is the electron chemical potential) is the energy required to add one hole to the system. In general, increased holes concentration increases the average hole-hole repulsion per hole and hence increases $-\mu$ if the hole distribution is spatially uniform. Therefore, the absence of change in $-\mu$ with hole doping suggests that there is no increase in the average hole-hole repulsion with increasing hole concentration. This can be made possible for a system in which holes are segregated, e.g., in a stripe form. For $\delta \gtrsim 0.33$ there is large downward shift of μ with hole doping, indicating an increase in the hole-hole repulsion between the overdoped holes. Therefore, it is considered that the repulsive interaction between hole stripes becomes significant for $\delta > 1/3$, where the stable $\epsilon = 1/3$ stripe ordering cannot survive. It is interesting to note that the shift of μ for LSCO and LSNO in the overdoped region is the same in magnitude in spite of their quite different electronic properties, i.e., metallic *versus* insulating.

A small but finite jump of ~ 0.1 eV μ from $\delta = 0.30$ to $\delta = 0.33$ appears to exist, according to Fig. 3. This jump may be explained by the gap opening in the $\delta = 0.33$ material as observed by the optical conductivity measurements.¹¹ If the gap remains stable for a finite range of hole concentration around $\delta = 1/3$ due to the high stability of the $\epsilon = 1/3$ stripe, in going from $\delta \lesssim 1/3$ to $\delta \gtrsim 1/3$, μ should show a jump equal to the magnitude of gap. The jump of ~ 0.1 eV is smaller than the gap value of 0.26 eV estimated from the optical spectra.¹¹ The discrepancy can be explained by the different experimental methods because the optical measurements probe the direct (momentum-conserving) gap whereas the chemical potential shift probes the minimum gap (which may be indirect).

Figure 4 shows valence-band spectra of $\text{La}_{1.67}\text{Sr}_{0.33}\text{NiO}_4$ taken at 150, 200, and 289 K in order to study spectral changes above and below the charge-ordering temperature $T_{\text{CO}} = 240$

K. Here, the background has been subtracted assuming the secondary-electron cascade process¹² and the spectra have been normalized to the peak height at ~ -3 eV. It should be noted that the following interpretation of the spectra is almost independent of the normalization procedure.

Each spectrum near E_F in Fig. 4(b) shows no Fermi edge, which is consistent with the insulating behavior below room temperature.⁴ The intensity near E_F clearly changes between above (289 K) and below (150 and 200 K) T_{CO} although there are no significant changes in the wide range spectra shown in Fig. 4(a). It should be noted that the $d^8\bar{L}$ feature at ~ -1.5 eV is significantly broadened above T_{CO} . This broadening is much stronger than that expected from the temperature broadening between 289 and 200 K and seems to reflect the order-to-disorder transition of charge carriers at $T = T_{CO}$. The decrease of the intensity at E_F in going from 289 to 200 K would be due to the gap opening at T_{CO} caused by the charge ordering as observed in the optical conductivity.¹¹ On the other hand, there is little change in the intensity between 150 and 200 K, indicating that the spectral intensity is not much affected by the spin ordering across $T_N (= 190$ K). These results are consistent with the electrical resistivity,¹¹ which shows a large change between 200 and 289 K and little changes between 150 and 200 K.

In conclusion, we have observed that the chemical potential in $\text{La}_{2-x}\text{Sr}_x\text{NiO}_4$ shows a large (~ 1 eV/hole) downward shift with hole concentration in the high doping regime ($\delta \gtrsim 0.33$) while it shows no appreciable shift in the low doping regime ($\delta \lesssim 0.33$). We have explained this observation as due to a segregation of doped holes on a microscopic length scale when the hole concentration is lower than $\delta = 1/3$, where the stable $\epsilon = 1/3$ charge stripes are formed. In $\text{La}_{1.67}\text{Sr}_{0.33}\text{NiO}_4$, the photoemission spectra exhibit subtle changes across the charge ordering transition temperature $T_{CO} = 240$ K: the intensity at E_F vanishes below T_{CO} , consistent with the transport and optical properties.

The authors would like to thank Dr. Y. Aiura for useful advise in designing the sample holder. MS is indebted to H. Hayashi for collaboration in the initial stage of this work. This work was supported by a Special Coordination Fund from the Science and Technology of Japan and Agency and the New Energy and Industrial Development Organization (NEDO).

(1996)

- ³ J. M. Tranquada, B. J. Sternlieb, J. D. Axe, Y. Nakamura, and S. Uchida, *Nature* **375**, 561 (1995); J. M. Tranquada, J. D. Axe, N. Ichikawa, A. R. Moodenbaugh, Y. Nakamura, S. Uchida, *Phys. Rev. Lett.*, **338** (1997).
- ⁴ S-W. Cheong, H. Y. Hwang, C. H. Chen, B. Batlogg, L. W. Rupp, Jr., and S. A. Carter, *Phys. Rev. B* **49**, 7088 (1994).
- ⁵ S. H. Lee and S-W. Cheong, *Phys. Rev. Lett.* **79**, 2514 (1997).
- ⁶ H. Yoshizawa, T. Kakeshita, R. Kajimoto, T. Tanabe, and Y. Tokura, submitted to *Phys. Rev. Lett.*
- ⁷ A. Ino, T. Mizokawa, A. Fujimori, K. Tamasaku, H. Eisaki, S. Uchida, T. Kimura, T. Sasagawa and K. Kishio, *Phys. Rev. Lett.* **79**, 2101 (1997).
- ⁸ A. Ino, T. Mizokawa, K. Kobayashi, A. Fujimori, T. Sasagawa, T. Kimura, K. Kishio, K. Tamasaku, H. Eisaki, and S. Uchida, *Phys. Rev. Lett.* **81**, 2124 (1998).
- ⁹ M. Oda, K. Hoya, R. Kubota, C. Manabe, N. Momono, T. Nakano, and M. Ido, *Physica C* **281**, 135 (1997).
- ¹⁰ K. Yamada, C. H. Lee, K. Kurahashi, J. Wada, S. Wakimoto, S. Ueki, H. Kimura, Y. Endoh, S. Hosoya, G. Shirane, R. J. Birgeneau, M. Greven, M. A. Kastner and Y. J. Kim, *Phys. Rev. B* **57**, 6165 (1998).
- ¹¹ T. Katsufuji, T. Tanabe, T. Ishikawa, Y. Fukuda, T. Arima and Y. Tokura, *Phys. Rev. B* **54**, 14230 (1996).
- ¹² Xiaomei Li and V. E. Henrich, *J. Electron Spectrosc. Relat. Phenom.* **63**, 253 (1993).

TABLE I. Chemical compositions of the $\text{La}_{2-x}\text{Sr}_x\text{NiO}_{4+y/2}$ samples studied in the present work. $\delta = x + y$ gives the hole concentration. No iodimetric titration was made for the $x = 0$ sample.

δ	0	0.22	0.23	0.30	0.33	0.34	0.50
x	0	0.10	0.20	0.30	0.33	0.36	0.50
y	0	0.12	0.03	0.00	0.00	-0.02	0.00

* To whom correspondence should be sent.

¹ J. M. Tranquada, D. J. Buttrey and V. Sachan, *Phys. Rev. B* **54**, 12318 (1996).

² J. Zaanen and P. B. Littlewood, *Phys. Rev. B* **50**, 7222 (1994); J. Zaanen and A. M. Oleś, *Ann. Physik* **5**, 224

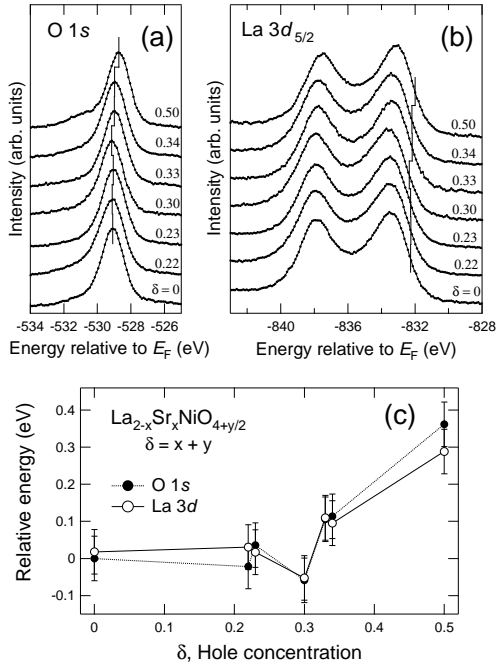


FIG. 1. O 1s (a) and La 3d_{5/2}(b) core-level spectra of La_{2-x}Sr_xNiO_{4+y/2} taken at $h\nu = 1253.6$ eV. The hole concentration is given by $\delta = x + y$. Vertical lines indicate the energy shift of the spectra (see text). (c) Energy shifts of the O 1s and La 3d spectra as functions of hole concentration.

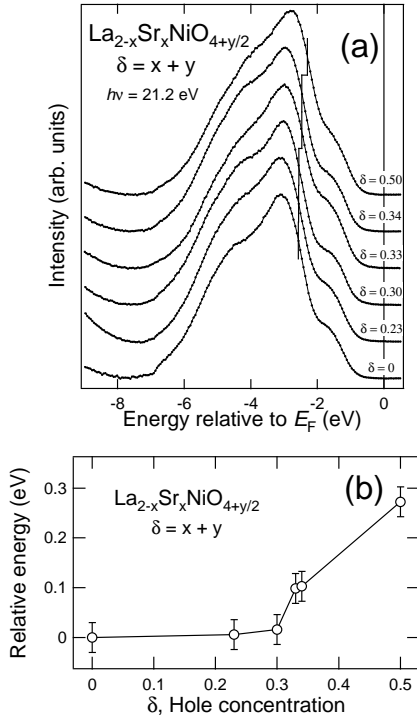


FIG. 2. (a) Valence-band spectra of La_{2-x}Sr_xNiO_{4+y/2}. Vertical lines indicate the position at 3/4 height of the non-bonding O 2p peak on the lower binding-energy side. (b) Energy shift of the non-bonding O 2p peak in the valence-band spectra as a function of hole concentration.

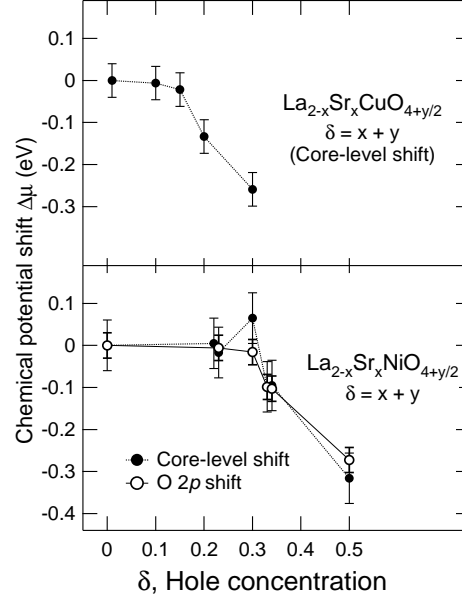


FIG. 3. (a) Chemical potential shift $\Delta\mu$ in La_{2-x}Sr_xNiO_{4+y/2} as a function of hole concentration δ . Solid circles are $\Delta\mu$ deduced from the average shift of the O 1s and La 3d XPS. Open circles indicate $\Delta\mu$ deduced from the shift of the non-bonding O 2p peak in the valence-band UPS. The UPS data for $\delta = 0$ was taken at 230 K, and the others at 150 K. (b) Chemical potential shift $\Delta\mu$ in La_{2-x}Sr_xCuO₄ as a function of hole concentration δ (taken from Ref. 7).

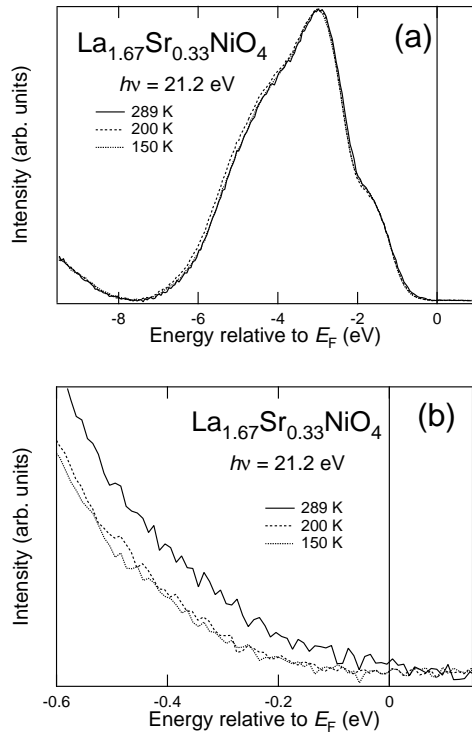


FIG. 4. Valence-band spectra of $\text{La}_{1.67}\text{Sr}_{0.33}\text{NiO}_4$ taken at 150, 200, and 289 K in a wide energy range (a) and near the chemical potential (b).